3-бөлім	Раздел 3	Section 3
Механика	Механика	Mechanics

A.Abdidin[1,3] (iD), **A.Kereikulova**[1,3] (iD), **A.Toleukhanov**[2] (iD), **O.Botella**[3] (iD), **A.Kheiri**[3] (iD), **Ye.Belyayev**[1*] (iD)

[1]Al-Farabi Kazakh National University, Kazakhstan, Almaty
[2]Satbayev University, Kazakhstan, Almaty
[3]University de Lorraine, CNRS, LEMTA, France, Nancy
*e-mail: yerzhan.belyaev@kaznu.edu.kz; yerzhan.belyayev@gmail.com

TWO-DIMENSIONAL CFD ANALYSIS OF A HOT WATER STORAGE TANK WITH IMMERSED OBSTACLES

A comprehensive study was conducted to develop a two-dimensional mathematical model for a thermal storage tank containing internal disk-shaped obstacles. This model, incorporating appropriate initial and boundary conditions, was solved using the built-in solvers of the licensed COMSOL Multiphysics 5.6 software. The COMSOL model demonstrated a maximum deviation of 2.2% from experimental results and even smaller discrepancies compared to ANSYS Fluent, validating its accuracy in describing the charging and discharging processes of a sensible heat storage tank with internal obstacles. Using this validated algorithm, numerical studies were performed to analyse temperature distribution and performance indicators for three distinct tank configurations. Among these configurations, the storage tank with a middle disk consistently exhibited superior performance. This tank achieved the highest mixing efficiency, as evidenced by smoother variations in the Richardson number and a more uniform temperature distribution. It also attained the highest capacity ratio (90.12%) and exergy efficiency (81.67%), indicating its effectiveness in heat retention and the quality of stored thermal energy. Furthermore, it demonstrated the highest charging efficiency at 67.51%, highlighting its ability to store incoming heat more effectively. These findings establish the tank with a middle disk as the most efficient configuration for thermal energy storage and uniform temperature distribution.

Key words : Sensible Heat Storage, Thermal Energy, Immersed Obstacles, Water Tank, CFD.

А.Н.Абдидин[1,3], А.Е.Керейкулова[1,3], А.Ә.Толеуханов[2], О.Ботелла[3], А.Хэйри[3], Е.К.Беляев[1*]
[1]әл-Фараби атындағы Қазақ Ұлттық университеті, Қазақстан, Алматы қ.
[2]Сәтбаев университеті, Қазақстан, Алматы қ.
[3]Лотарингия университеті, CNRS, LEMTA, Франция, Нанси қ.
*e-mail: yerzhan.belyaev@kaznu.edu.kz; yerzhan.belyayev@gmail.com

Су астындағы кедергілері бар екі өлшемді ыстық су сақтау бағын CFD талдау

Ішкі диск тәрізді кедергілері бар жылу сақтайтын бакты екі өлшемді математикалық моделін жасау бойынша кешенді зерттеу жүргізілді. Бұл модель тиісті бастапқы және шекаралық шарттарды ескере отырып, лицензияланған COMSOL Multiphysics 5.6 бағдарламалық жасақтамасының кіріктірілген шешушілерінің көмегімен шешілді. COMSOL моделі эксперимент нәтижелерінен максималды 2,2% ауытқуды және ANSYS Fluent-пен салыстырғанда одан да аз сәйкессіздіктерді көрсетті, бұл оның ішкі кедергілері бар сезілентін жылу сақтау бағының зарядтау және разрядтау процестерін сипаттаудағы дәлдігін растады. Осы тексерілген алгоритмді пайдалана отырып, бактың үш түрлі конфигурациясы үшін температураның таралуын және өнімділік көрсеткіштерін талдау үшін сандық зерттеулер жүргізілді. Осы конфигурациялардың ішінде ортаңғы дискісі бар сақтау бағы үнемі жоғары өнімділікті көрсетті. Бұл бак араластырудың ең жоғары тиімділігіне қол жеткізді, бұл Ричардсон санының біркелкі өзгеруімен және температураның біркелкі таралуымен дәлелденді.
Ол сондай-ақ ең жоғары сыйымдылық коэффициентіне (90,12%) және эксергия тиімділігіне (81,67%) қол жеткізді, бұл оның жылуды сақтаудағы тиімділігін және жинақталған жылу энергиясының сапасын көрсетеді. Сонымен қатар, ол зарядтаудың ең жоғары тиімділігін көрсетті - 67,51%, бұл оның кіретін жылуды тиімдірек сақтау қабілетін көрсетеді. Бұл нәтижелер жылу энергиясын сақтау және температураны біркелкі таралуы үшін ең тиімді конфигурация ретінде ортаңғы дискі бар бакты көрсетті.

Түйін сөздер: Сезілетін жылуды сақтау, Жылу энергиясы, Су ішіндегі кедергілер, Су бағы, Есептеу гидродинамикасы (CFD).

А.Н. Абдидин[1,3], А.Е. Керейкулова[1,3] , А.Е. Толеуханов[2], , О. Ботелла[3], А. Хэйри[3],
Е.К. Беляев[1*]
[1]Казахский Национальный университет имени Аль-Фараби, Казахстан, г. Алматы
[2]Сәтбаев университеті, Казахстан, г. Алматы
[3]Университет Лотарингии, CNRS, LEMTA, Франция, г. Нанси
*e-mail: yerzhan.belyaev@kaznu.edu.kz; yerzhan.belyayev@gmail.com

Двумерный CFD-анализ бака для хранения горячей воды с погруженными препятствиями

Было проведено комплексное исследование для разработки двумерной математической модели бака для хранения тепла, содержащего внутренние препятствия в форме диска. Эта модель, включающая соответствующие начальные и граничные условия, была решена с использованием встроенных решателей лицензионного программного обеспечения COMSOL Multiphysics 5.6. Модель COMSOL продемонстрировала максимальное отклонение от экспериментальных результатов в 2,2% и еще меньшие расхождения по сравнению с ANSYS Fluent, что подтверждает ее точность в описании процессов зарядки и разрядки бака для хранения тепла с внутренними препятствиями. Используя этот проверенный алгоритм, были проведены численные исследования для анализа распределения температуры и показателей производительности для трех различных конфигураций баков. Среди этих конфигураций бак для хранения со средним диском неизменно демонстрировал превосходную производительность. В этом баке достигнута высочайшая эффективность перемешивания, о чем свидетельствуют более плавные колебания числа Ричардсона и более равномерное распределение температуры. Он также достиг самого высокого коэффициента полезного действия (90,12%) и эксергетического КПД (81,67%), что свидетельствует о его эффективности в области сохранения тепла и качества аккумулируемой тепловой энергии. Кроме того, он продемонстрировал высочайшую эффективность зарядки - 67,51%, что подчеркивает его способность более эффективно накапливать поступающее тепло. Эти данные свидетельствуют о том, что бак со средним диском является наиболее эффективной конфигурацией для накопления тепловой энергии и равномерного распределения температуры.

Ключевые слова: Ощущаемая тепловая энергия, Тепловая энергия, Погруженные препятствия, Бак для воды, Вычислительная гидродинамика (CFD).

1 Introduction

The efficient storage of thermal energy is crucial for optimizing the performance of renewable energy systems, particularly those that rely on solar thermal and geothermal sources. Hot water storage tanks play a vital role in these systems by storing excess thermal energy for later use, thereby enhancing energy efficiency and system reliability. However, the thermal stratification [1] within these tanks, which significantly impacts their performance, is influenced by various factors including tank geometry [2], insulation, and internal components [3].

In recent years, computational fluid dynamics (CFD) has emerged as a powerful tool for analyzing and optimizing the performance of thermal storage systems [4-5]. CFD enables detailed investigations into the flow dynamics, heat transfer mechanisms, and thermal stratification within hot water storage tanks [6]. By simulating different configurations and operating conditions, researchers can gain insights into the factors affecting thermal efficiency and develop strategies to enhance tank performance. Bouhal et al. [7] utilized CFD simulations with ANSYS Fluent software to investigate the performance of two hot water storage tank configurations. They evaluated performance indicators such as temperature evolution, Richardson number, and stratification number. These two configurations pertain to the arrangement of flat plates inside the tank and the orientation of the plate in the middle of the tank. They also differ in the configurations of the inlet and outlet nozzles. The major findings of the current analysis indicate that the optimal configuration for the first setup is a tank with two plates positioned at the middle and top. The tank with a 30° tilted plate demonstrates the best performance for the second setup. This conclusion is based on the significant values of the thermocline extent and stratification number and a Richardson number greater than 1, indicating that buoyancy forces dominate over mixing forces. This group of authors, Fertahi et al. [8], continued their work in this direction by conducting CFD analysis of a horizontal hot water storage tank used in evacuated tube collector (ETC) systems with heat pipes. The influence of the number of heat pipes on the temperature distribution, average temperature in the tank, and discharge efficiency was studied. An increase in the number of heat pipes resulted in an improvement in these indicators. Lou et al. [9] presented numerical and experimental studies to investigate the effect of internal disk-like ring-opening plates on sensible heat storage tank performance. Unlike the previous works, these disks have ring-shaped holes through which the HTF can pass. CFD simulation-based optimization for the so-called Ring-Opening Plate Distributors (ROPDs) was presented using ANSYS Fluent. The reported results show that charging and discharging efficiencies improved by 14.5% and 19.8%, respectively, compared to the conventional storage tank. In addition to the internal geometric configurations, studies are focusing on the external geometric configurations of the tank. Shafieian et al. [10] used unsteady 3D numerical simulations with ANSYS Fluent to test the effects of four different inlet and outlet configurations for the storage tank HTF. For the first configuration with a single inlet and a single outlet, the effects of varying mass flow rates on the thermal performance of a simple tank were investigated. The results indicate that higher mass flow rates degrade the thermocline and thermal stratification, which are desirable. To mitigate the adverse effects of inlet jet mixing with stagnant fluid, the mass flow rates were evenly distributed between two inlet ports in the second configuration. This model demonstrated improved heat transfer performance compared to the previous model. In the

third configuration, the inlet port was replaced with a circular truncated cone-shaped diffuser, while in the fourth configuration, the orientation of this diffuser relative to the horizontal axis was examined. The effects of the diffuser aspect ratio were analyzed at fixed mass flow rates. The results indicate that smaller aspect ratios enhance tank performance, whereas larger aspect ratios degrade performance due to a strongly adverse pressure gradient within the diffuser. This adverse pressure gradient leads to high-speed core flow, which contradicts the intended function of the diffuser. Additionally, altering the inlet orientation was found to be less effective compared to the previously discussed modifications. In another study, Kong et al. [11] conducted 3D numerical simulations for a hot water storage tank equipped with an internal cylinder designed to enhance the uniform distribution of heated fluid within the tank. This paper investigates the impact of the inner cylinder's design and operating parameters on water flow characteristics, thermal stratification, and overall performance of a hot water storage tank during the heat charging process in thermal energy systems. It was reported that the presence of an internal cylinder with openings significantly enhances thermal stratification in the tank by stabilizing the thermocline and prolonging the upper warm layer.

The cylinder acts as a uniform diffuser, minimizing the impact of turbulence and heat conduction on the tank body, and ensuring a more stable temperature distribution. Kumar and Singh [12] conducted a numerical simulation to analyze the charging behavior of a thermal storage tank equipped with two integrated coil heat exchangers, which receive heat from distinct sources such as a solar thermal collector and a heat pump. The simulations, performed using ANSYS Fluent, involved calculating axial temperature evolution, dimensionless stratification, and Richardson numbers for various operational scenarios. The results indicate that thermal stratification within the tank is influenced by the positioning of the heating sources. Specifically, the degree of stratification is enhanced when the heat exchanger coil installed in the upper portion of the tank is operational, both during the charging process and in continuous delivery mode. The aforementioned configurations primarily focus on the HTF inlet and outlet arrangements in the tank, as well as the charging modes involving additional built-in heat exchangers. However, the heat distribution within the tank during periods when it is neither charging nor discharging is also a crucial aspect of interest. Buoyancy-induced thermal stratification is a spontaneous phenomenon arising from standby periods of hot water tanks [13]. Li et al. [13] proposed a semi-analytical method for assessing buoyancy-induced thermal stratification, eliminating the need for numerical simulation procedures. Li et al.'s semi-analytical method, which derives an explicit water temperature function based on tank height and time by modifying the energy balance equation, successfully compensates for convection effects through an amplification factor. Their numerical study demonstrates a strong analogy between buoyancy-induced thermal stratification and bottom-initiated heat conduction, reinforcing the validity of the proposed method.

The brief literature review indicates that the majority of studies focus on the numerical analysis of thermal performance in hot water tanks using ANSYS Fluent. Additionally, many of these studies concentrate on a limited set of performance indicators. This study focuses on a two-dimensional CFD analysis of a hot water storage tank with immersed obstacles using COMSOL Multiphysics 5.6 [14]. The validation of the numerical calculation algorithm based on COMSOL is performed by comparing it with experimental data and calculations

from other authors documented in the literature [7]. Additionally, a comprehensive numerical evaluation of a wide range of tank performance indicators is conducted. The proposed research introduces novel insights and lays the foundation for future investigations by the authors into various sensible heat storage tank configurations.

In summary, this research paper presents a comprehensive two-dimensional CFD analysis of a hot water storage tank with immersed obstacles, highlighting the potential benefits and challenges associated with their use. The study aims to advance our understanding of thermal stratification and heat transfer mechanisms in such systems, ultimately contributing to the enhancement of renewable energy storage technologies.

2 Physical model

The physical model for this study consists of a cylindrical hot water storage tank equipped with a series of immersed obstacles designed to enhance thermal stratification. The tank dimensions, material properties, and insulation characteristics are specified to closely resemble typical thermal storage systems used in solar and geothermal applications. The obstacles within the tank are strategically placed to disrupt the natural convection currents, thereby promoting a more uniform temperature distribution and minimizing thermal mixing. The physical model includes detailed geometric representations of these obstacles, which may vary in shape, size, orientation, and placement. Additionally, the model accounts for the boundary conditions, such as the heat flux at the tank walls, initial temperature distribution, and inlet/outlet fluid dynamics. This comprehensive physical representation forms the basis for the subsequent computational fluid dynamics (CFD) simulations, enabling an accurate analysis of the thermal performance and energy efficiency of the hot water storage tank under various operating conditions.

As stated in the Introduction section, this paper examines a hot water storage tank utilizing sensible heat storage. These studies serve as preliminary calculations for future applications in thermal storage tanks incorporating phase change materials. The primary objective of this study is to investigate the impact of metal disk obstacles on the distribution of heat transfer fluid (HTF) within a heat storage tank. The inlet and outlet configurations for the HTF consist of narrower tubes, as depicted in Figure 1. Figure 1 presents three configurations of hot water storage tanks, where the external tank dimensions are consistent across all cases. The tank height is H=800 mm, the diameter is D=400 mm, and the diameter of the inlet and outlet orifices for the HTF flow is b=20 mm. The configurations of metal disk obstacles are as follows: Tank 1 - Bottom-Top, Tank 2-Bottom-Middle-Top, and Tank 3-Middle, with three metal disks fully integrated inside the storage tank, as illustrated in Figure 1. The objective is to investigate the effect of the obstacle's positions on thermal stratification within the standard storage tank. For all three cases, thin disks with a diameter of d=300 mm are used. The orientation of the disks is not varied; in all cases, the disks are positioned horizontally. Only the heat accumulation tank charging mode is considered, where the inlet is at the bottom of the tank and the outlet is at the top. The inlet HTF temperature is 50 °C, and the initial temperature of the water inside the tank is 15 °C. The HTF inlet velocity is 0.1694 m/s. The tank walls and disks are both constructed from stainless steel. The modeling assumes that the tank walls are perfectly insulated, with no heat loss.

Table 1: Geometries and operating conditions

Parameter	Value
Diameter D (mm)	400
Height H (mm)	800
Diameter d (mm)	300
Diameter b (mm)	20
Hot temperature T_{in} (°C)	50
Cold temperature T_{ini} (°C)	15
Inlet velocity u_{in} (m/s)	0.1694
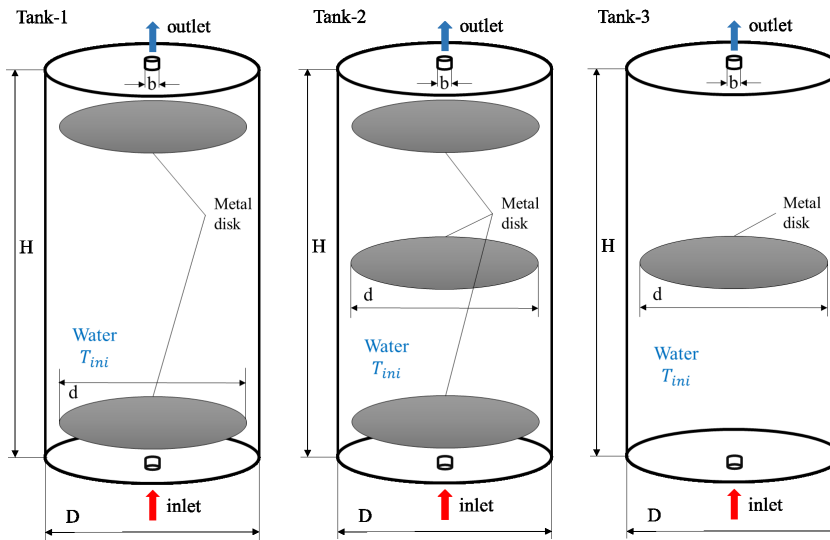
Figure 1: Schematic configurations of the storage tank with different disk positions.

3 Mathematical model

3.1 CFD model

This section provides a comprehensive framework for analysing the thermal and fluid dynamics within the hot water storage tank. This section details the fundamental assumptions and equations that underpin the simulation of heat transfer and fluid flow. By establishing a set of key assumptions, the model aims to accurately represent the behaviour of the system under different configurations, particularly focusing on the impact of immersed obstacles on thermal stratification. The following describes the basic assumptions that govern the mathematical formulation, followed by the specific equations used to model the system's transient heat and fluid dynamics. The unsteady two-dimensional flow models for heat transfer within a standard storage tank are based on the following assumptions: the working fluid is treated as incompressible; the thermophysical properties of the fluid are considered constant, except for density variations due to temperature changes, which are accounted for using the Boussinesq approximation to model thermal buoyancy effects;the fluid is assumed to be Newtonian; viscous dissipation effects are considered negligible; the fluid motion is

assumed to be laminar and two-dimensional.

The transient fluid dynamic and thermal fields are described using the two-dimensional forms of the Navier-Stokes and energy equations, incorporating the effects of gravity. Consequently, the governing equations are formulated based on these assumptions. The HTF is described by the system of 2D Navier-Stokes equations for an incompressible fluid. Continuity is described by Equation (1):

$$\frac{\partial u}{\partial x} + \frac{\partial v}{\partial x} = 0, \tag{1}$$

Conservation of momentum in two directions is described by the following equation:

$$\begin{cases} \rho_f \dfrac{\partial u}{\partial t} + \rho_f \left(u\dfrac{\partial u}{\partial x} + v\dfrac{\partial u}{\partial y} \right) = -\nabla p_f + \mu_f \left(\dfrac{\partial^2 u}{\partial x^2} + \dfrac{\partial^2 u}{\partial y^2} \right) \\ \rho_f \dfrac{\partial v}{\partial t} + \rho_f \left(u\dfrac{\partial v}{\partial x} + v\dfrac{\partial v}{\partial y} \right) = -\nabla p_f + \mu_f \left(\dfrac{\partial^2 v}{\partial x^2} + \dfrac{\partial^2 v}{\partial y^2} \right) + F_y \end{cases} \tag{2}$$

here the index f - is an indicator of the HTF, and gravity is considered in the direction y. Energy equation describing the heat exchange process is defined as follows:

$$\rho_f C_{p,f} \frac{\partial T}{\partial t} + \rho_f C_{p,f} u \nabla T = \nabla(k \nabla T) \tag{3}$$

For fluid flow, boundary conditions (BC) on solid surfaces such as the inner wall of the vessel and the surfaces of metal discs. In addition, it is assumed that the storage tank is completely isolated, which is determined by the formula:

$$-n(-k\nabla T) = 0 \tag{4}$$

Where n is the normal vector to the heat transfer surface. Thus, heat transfer is carried out only with the help of inlet and outlet pipes. There is a heat exchange inside the tank which can be described as:

$$-n(-k\nabla T) = \rho_f \Delta H_f \, \mathbf{u} \cdot \mathbf{n} \tag{5}$$

$$\Delta H_f = \int_{T_0}^{T} C_{p,f} \, dt \tag{6}$$

3.2 Initial and boundary conditions

This subsection provides a detailed description of the parameters and constraints applied to the model to ensure accurate and realistic simulations. Initial conditions define the starting state of the system, including temperature distributions and fluid velocities, while boundary conditions specify the constraints at the edges of the computational domain. Together, these conditions establish the framework within which the governing equations are solved, ensuring that the model reflects the physical behavior of the system under study. This section is crucial for setting up the simulation and obtaining reliable results that align with experimental or

theoretical expectations. For the system shown in Figure 2 (Tank 3), the initial and boundary conditions can be defined as follows:

Initial Temperature of Water (T_{ini}):

$$T(x, y, t = 0) = T_{\mathrm{ini}} = 15\,^{\circ}\mathrm{C} \tag{7}$$

Inlet: Velocity Boundary Condition:

$$u = u_{\mathrm{in}} = 0.1694 \text{ m/s} \tag{8}$$

Temperature Boundary Condition:

$$T = T_{\mathrm{in}} = 50\,^{\circ}\mathrm{C} \tag{9}$$

Outlet: Pressure Boundary Condition:

$$P_0 = 0 \tag{10}$$

Tank Walls ("No Slip")

$$u = v = 0 \tag{11}$$

Temperature Boundary Condition:

$$\frac{dT}{dx} = 0 \tag{12}$$

which indicates no heat flux through the walls. The diagram in Figure 2 corresponds to the Tank 3 configuration as shown in Figure 1. For the first two tank configurations, similar initial and boundary conditions are applied, considering a larger number of disks.

3.3 Performance indicators

The thermal energy storage system performance can be evaluated through two primary methodologies: graphical (visual) techniques and performance indicator (quantitative) approaches. Graphical techniques involve CFD analyzing temperature and velocity contours within the storage tank, providing detailed insights into local thermal and fluid dynamics. However, while these techniques offer valuable visual information, they do not yield direct quantitative assessments of the system's overall effectiveness. In contrast, performance indicator approaches calculate specific metrics to assess the system's operational efficiency and effectiveness. To achieve a comprehensive evaluation of the system's performance, it is essential to integrate both graphical analysis and performance indicators, thereby ensuring a thorough assessment of the system's behavior and effectiveness.

Based on the literature, performance indicators for thermal energy storage systems can be classified according to their adherence to the principles of thermodynamics. Indicators aligned with the first law of thermodynamics are designed to quantify the amount of thermal energy stored in the system, reflecting the total energy balance. Conversely, indicators consistent with the second law of thermodynamics assess the quality of the stored energy, providing insights into the efficiency and effectiveness of the energy storage process. By distinguishing between

these two categories of indicators, a more comprehensive evaluation of both the quantity and quality of the thermal energy stored can be achieved. The capacity ratio σ quantifies the fraction of the total thermal energy (E^V_{stored}) retained at the conclusion of the charging phase relative to the system's maximum thermal energy storage capacity ($E_{\text{max\_stored}}$) [15]:

$$\sigma = \frac{E^V_{\text{stored}}}{E_{\text{max\_stored}}} \tag{13}$$

$$E^V_{\text{stored}} = \int_V \rho_f C_{p,f}(T - T_c)\, dV \tag{14}$$

$$E_{\text{max\_stored}} = \rho_f C_{p,f} V_{\text{tank}}(T_h - T_c) \tag{15}$$

where T - current water temperature,T_{h} - final uniform water temperature along the height of the tank.$C_{p,f}$ - specific heat, ρ_f - fluid density,V_{tank} - tank volume without metal disks.
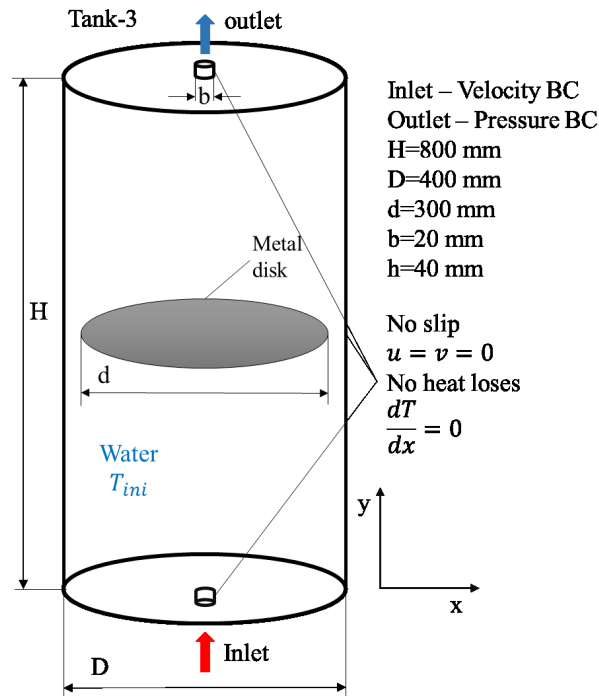
Figure 2: Schematic representation of initial and boundary conditions.

By applying the principles of the first and second laws of thermodynamics, exergy quantifies both the quantity and quality of the thermal energy stored in storage tanks [16]. The exergy of a sensible heat storage tank quantifies the potential to do work based on the thermal energy stored and the temperature difference relative to the ambient environment. In [17], exergy efficiency is defined as the ratio of the actual exergy of the storage tank at

the end of the charging process to the ideal exergy that the tank could have achieved under ideal conditions at the same point in time:

$$\eta_{\text{exergy}} = \frac{\text{Exergy}_{\text{real}}}{\text{Exergy}_{\text{ideal}}}\bigg|_{\text{at the end of charging process}} \tag{8}$$

$$\text{Exergy}_{\text{real}} = \int_V \left[\rho_f C_{p_f} (T - T_a)\, dV \right] - \int_V \left[\rho_f C_{p_f} T_a \ln\left(\frac{T}{T_a}\right) dV \right] \tag{9}$$

$$\text{Exergy}_{\text{ideal}} = \rho_f C_{p_f} V_{\text{tank}} \left[(T_{\text{h}} - T_{\text{a}}) - T_{\text{a}} \ln\left(\frac{T_h}{T_a}\right) \right] \tag{10}$$

where T_{a} - the ambient temperature. To mitigate operational problems associated with overheating or undercooling phenomena [18-20], it is crucial to select appropriate charging/discharging cut-off temperatures. This temperature defines the threshold at which the charging or discharging process is halted. Typically, values of $T_{(20\%)}$ and $T_{(80\%)}$ are employed as the cut-off temperatures for charging and discharging, respectively [21]:

$$T_{(x\%)} = T_c + x\% \cdot (T_h - T_c) \tag{19}$$

where the temperatures T_{h} and T_{c} correspond respectively to the hot and cold extremes.

In practical applications, a significant increase in the temperature of the heat transfer fluid exiting the storage system over time is anticipated to positively influence the capacity ratio. To assess this effect, a dimensionless parameter known as the tail factor (τ) is derived from the temporal temperature profile of the outlet fluid. The tail factor is independent of the thermal properties of the HTF, the system's geometry, and the operational conditions, rendering it an effective metric for evaluating the quality of the stored thermal energy. Moreover, it facilitates the comparison of different storage systems. The tail factor is computed using the following formula:

$$\tau = \frac{T_{(80\%)} - T_{(20\%)}}{t_{(80\%)} - t_{(20\%)}} \tag{20}$$

where $t_{(20\%)}$ and $t_{(80\%)}$ represent the times at which the outlet temperature of the tank reaches $T_{(20\%)}$ and $T_{(80\%)}$, respectively.

The ratio of the integral of net stored energy to the integral of total inlet energy is termed charging efficiency (η_{ch}). In contrast, the ratio of the integral of net extracted energy to the integral of initially stored energy is termed discharging efficiency (η_{dis}). In mathematical form it looks like this:

$$\eta_{\text{ch}} = \frac{E_{\text{in}} - E_{\text{out}}}{E_{\text{stored}}^t} = \frac{\int_{t_0}^t \dot{m}_f C_{p_f}(T_{\text{in}} - T_{\text{out}})\, dt}{\int_{t_0}^t \dot{m}_f C_{p_f}(T_{\text{in}} - T_{\text{ini}})\, dt} \tag{21}$$

$$\eta_{\text{dis}} = \frac{E_{\text{out}} - E_{\text{in}}}{E_{\text{stored}}^t} = \frac{\int_{t_0}^t \dot{m}_f C_{p_f}(T_{\text{out}} - T_{\text{in}})\, dt}{E_{\text{stored}}^t} \tag{22}$$

where T_{in} and T_{out} are the inlet and outlet temperatures of the HTF, respectively, C_{p} is the temperature-dependent specific heat of the HTF, and $\dot{m}_f$ is the mass flow rate. Another parameter is the Richardson number (Ri) for the storage tank, which indicates the relationship between natural and forced convection in the liquid. It is defined as the ratio of the potential energy associated with temperature stratification to the kinetic energy associated with fluid motion. This number is used to evaluate the degree of stratification in storage tanks: a high Richardson number indicates the dominance of natural convection and good stratification, while a low value indicates the dominance of forced convection and more uniform mixing of the liquid. The Richardson number is calculated using the following formula:

$$\text{Ri} = \frac{g\beta H(T_{\text{top}} - T_{\text{bottom}})}{u_{\text{in}}^2} \tag{23}$$

where T_{top} and T_{bottom} are the temperatures at the top and bottom of the tank, respectively. u_{in} is the inlet velocity of the HTF.

4 Calculation model

The computational analysis was conducted using COMSOL Multiphysics 5.6 software [14], a robust tool for solving complex fluid dynamics and heat transfer problems. The geometry of the hot water storage tank, along with the immersed obstacles, was modeled in a 2D domain to simplify the computational effort while capturing essential physical behaviors. The governing equations for fluid flow and heat transfer were implemented using the finite element method (FEM) provided by COMSOL. The incompressible Navier-Stokes equations were solved for fluid motion, coupled with the energy equation to account for heat transfer. Boundary conditions were applied to simulate the inlet and outlet of the HTF, as well as the insulated tank walls (see subsection 3.2). The simulations were performed in an unsteady state to capture the transient nature of the heat storage process. During the calculations, the effect of buoyancy was initially considered using the Boussinesq model. However, it was found that the results were not significantly affected by buoyancy. Consequently, for simplicity, the buoyancy effect was neglected in the final analysis. The mesh was refined iteratively to ensure accuracy and convergence of the results. The post-processing tools within COMSOL Multiphysics were utilized to visualize temperature distributions, velocity fields, and other relevant parameters, providing comprehensive insight into the system's thermal and fluid dynamics.

4.1 Mesh parameters

A structured grid was utilized, with the final mesh consisting of approximately 7,700 to 10,775 elements, depending on the storage tank configuration considered. The cells near the outlet, inlet apertures, metal disks, and walls were sufficiently small to accurately capture the complex flow structure, as illustrated in Figure 3. For the 2D mesh model, the software automatically generated rectangular cells and triangular cells in the solid wall areas. The discretization of the system of equations, based on the FEM, was implemented on these cells. The details of the computational grids are presented in Table 2.

Table 2: Mesh properties

Parameter	Tank-1	Tank-2	Tank-3
Mesh type	Basic 2D shapes	Basic 2D shapes	Basic 2D shapes
Number of elements	8720	10775	7700
Number of rectangular cells	956	1150	752
Number of triangular cells	7764	9625	6948
Min element quality	0.214	0.213	0.214
Mesh area (m^2)	0.3196	0.3190	0.3202

4.2 Computational algorithm

The computational algorithm employed in this study utilizes COMSOL Multiphysics 5.6 [14], a robust simulation software capable of handling complex multiphysics problems. The modeling process begins with the creation of a geometrical representation of the hot water storage tank and the immersed obstacles.

The next step involves selecting the materials and working fluids used in the simulation. Subsequently, the appropriate solvers built into the software are chosen to account for the physics of the flow, such as laminar flow and heat transfer in fluids, along with the initial and boundary conditions. This is followed by the construction of the computational grid. The final step is selecting a solver, either stationary or time-dependent, depending on the nature of the simulation. Figure 4 provides a detailed step-by-step guide for solving a problem in COMSOL Multiphysics 5.6 software.
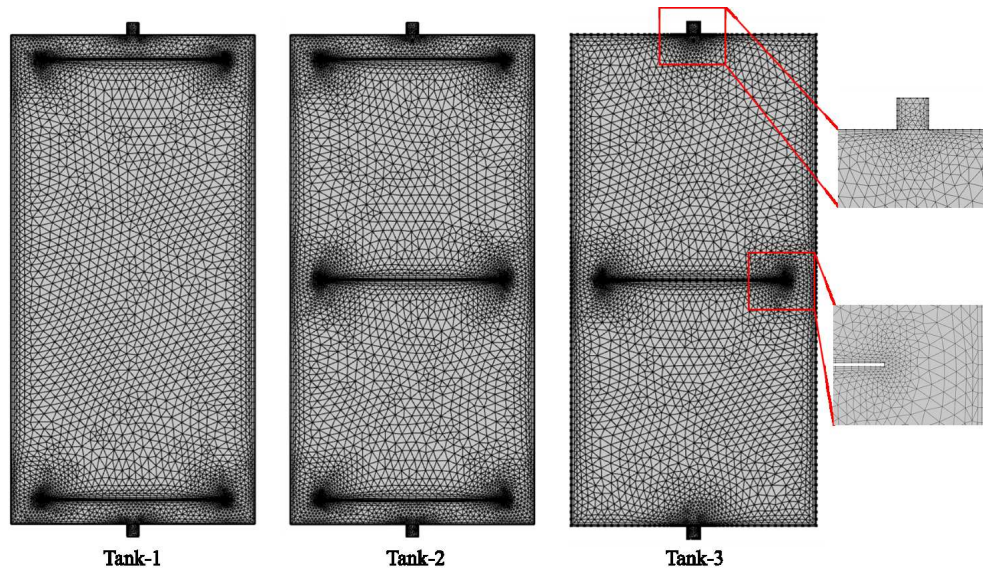
Figure 3: 2D computational grid for the specified configurations
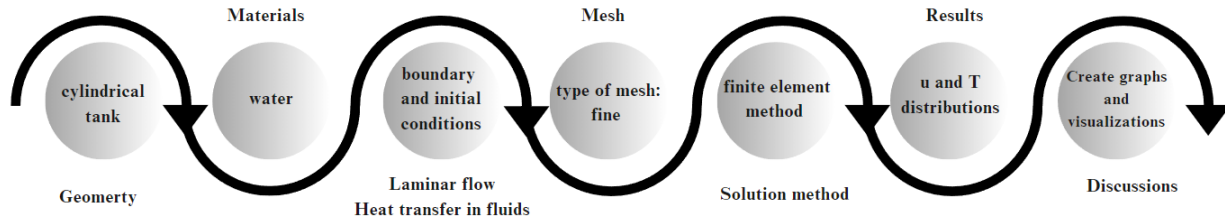
Figure 4: Roadmap for solving a problem using COMSOL Multiphysics

4.3 Model validation

To validate the numerical calculation algorithm, a comparison was made between the obtained results and the experimental data of Zachar et al. [22]. Additionally, the numerical results were compared with those obtained using ANSYS Fluent by Bouhal et al. [7]. The geometric configuration of the experimental prototype corresponds to the third tank presented in Figure 1, with the metal disk located at a height of 40 mm from the bottom of the tank. Figure 5 illustrates the configuration used for validating the calculations.
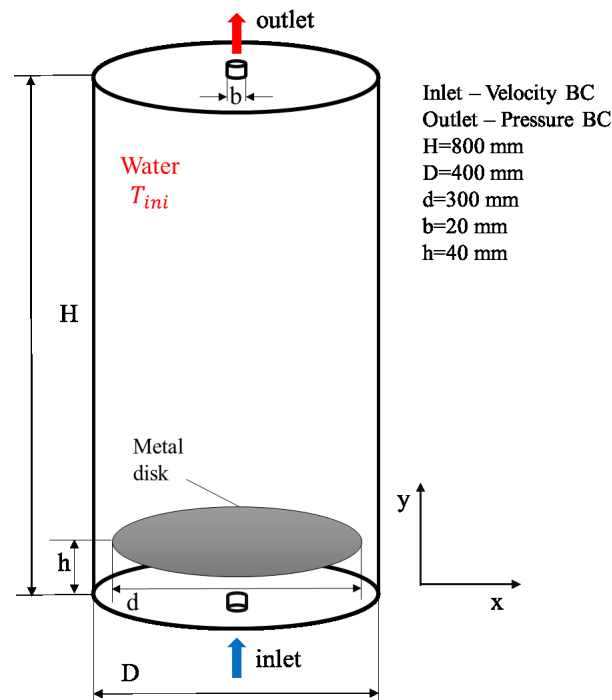
Figure 5: Geometric configuration for validation purposes

To compare the obtained data, the dimensionless HTF temperature T^* is introduced, as

described in reference [7]:

$$T^* = \frac{T - T_{\text{in}}}{T_{\text{ini}} - T_{\text{in}}} \tag{24}$$

$$\text{error} = \frac{T^*_{\text{exp}} - T^*_{\text{num}}}{T^*_{\text{exp}}} \cdot 100\% \tag{25}$$

In the experimental setup, the initial water temperature in the tank was 50 °C, while the inlet temperature was 20 °C, and the inlet HTF flow rate was 0.26 kg/s. Figure 6 illustrates the effect of axial position on the variation of the dimensionless fluid temperature T^*.

Calculations were performed for these conditions up to 300 seconds, and distributions of the dimensionless temperature T^* were obtained. The data presented in Figure 6 were extracted from the T^* distribution at 140 seconds. This time was chosen because stratification of the HTF is observed at heights ranging from 200 mm to 600 mm. Each point on the graph indicates that T^* is constant within that specific thickness along the height of the tank.

As shown in Figure 6, the thicknesses exhibit more significant differences than the temperatures. The exact match of thicknesses is not critical for the analysis due to differing modeling approaches and computational meshes between the two software packages. The agreement in dimensionless temperature T^* is more important. According to this parameter, the maximum difference between the experimental results and COMSOL is 2.2%, while the difference between COMSOL and ANSYS is even smaller. This comparison is detailed in Table 3. Based on the verification analysis of the computational model, it can be concluded that the calculation algorithm in COMSOL software accurately describes the charging and discharging processes of a sensible heat storage tank with obstacles.

Table 3: Comparison of validation results.

Experimental results		COMSOL Multiphysics results		error
T^*	Positions (cm)	T^*	Positions (cm)	
0.13	0.24	0.13	0.32	0
0.137	0.24	0.136	0.34	0.73%
0.2	0.25	0.2	0.38	0
0.27	0.26	0.27	0.4	0
0.37	0.28	0.37	0.42	0
0.54	0.3	0.54	0.44	0
0.69	0.32	0.69	0.48	0
0.84	0.35	0.84	0.49	1.2%
0.91	0.37	0.89	0.5	2.2%
0.98	0.41	0.99	0.53	1.1%
0.99	0.52	0.99	0.55	0
1	0.55	1	0.575	0
1	0.55	1	0.6	0
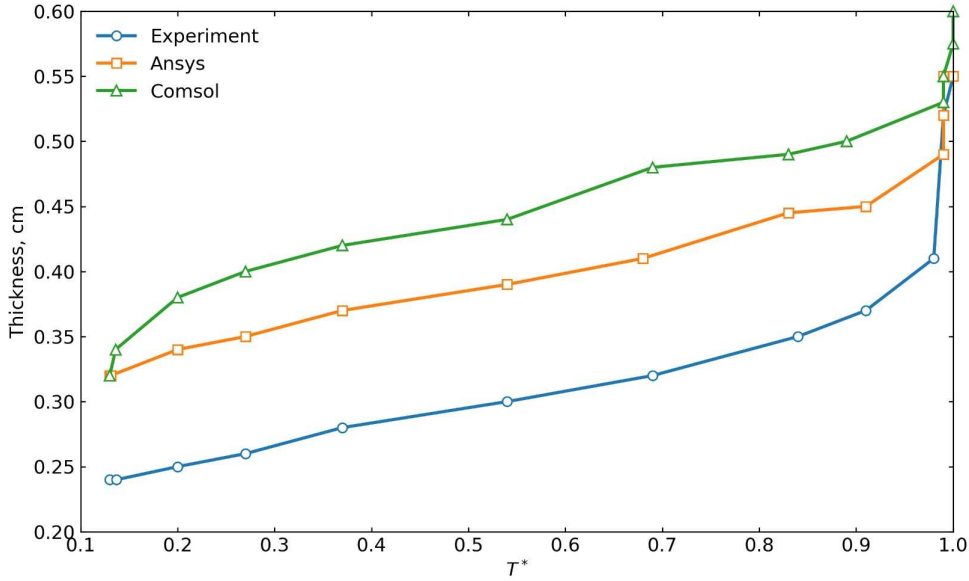
Figure 6: Comparison between numerical dimensionless temperatures and the evaluation of relative error.

5 Results and discussion

This section presents the findings from the two-dimensional CFD analysis of a hot water storage tank with immersed obstacles. The analysis focuses on understanding the tank's thermal stratification and fluid dynamics during charging and discharging processes. The results include temperature distributions, flow patterns, and the impact of immersed obstacles on thermal storage efficiency. Performance indicators for the three tank configurations are discussed, and conclusions are drawn based on the simulation results.

Figure 7 shows temperature contours in degrees Celsius, taking into account the presence of metal disks. According to the calculation results, recirculation zones are observed in front of and behind the obstacles. The size of these recirculation zones depends on the location of the disks. For all three cases, the inlet fluid velocity is the same $u_{\mathrm{in}} = 0.1694 m/s$. The fluid enters from the bottom of the tank at a temperature of 50 °C, while the initial temperature of the water in the tank is 20 °C. For Tank 1, where the disks are located at the top and bottom, the maximum temperature is distributed along the walls of the tank. This is because as the HTF flows around the lower disk, the fluid flow is directed along the wall, resulting in a less intense mixing of warmer fluid with cooler fluid in the central part of the tank. The temperature distribution follows the vorticity profile, clearly forming two large vortices. According to the numerical data, the water temperature in the central part differs from the water temperature along the wall by 20-22%. Including an additional disk in the center of the tank, as in the Tank 2 configuration, resulted in an increase in the number of vortices but a decrease in their size. At the same time, a slight improvement in mixing is observed in the central part of the tank. It can be seen that the temperature near the central disk has increased, but in the central part of the vortices, the temperature remains the same as in the previous case. In this case, the lower disk greatly influences the distribution of the HTF

along the wall, and as a result, the central part of the tank does not heat up as quickly.
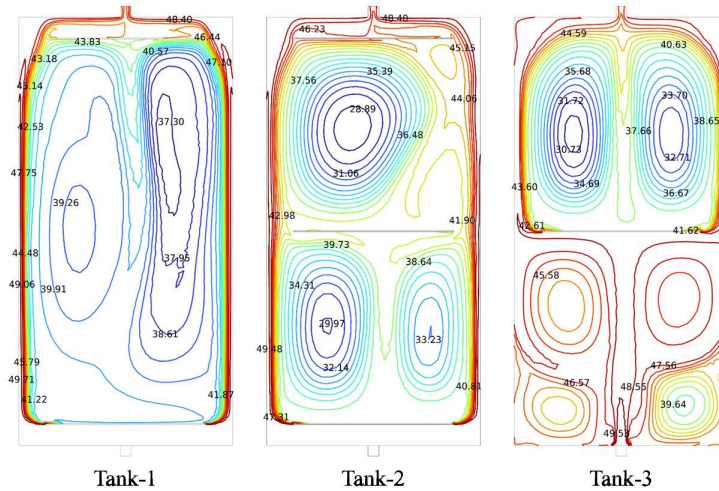
Figure 7: Temperature contours in degrees Celsius.

Now, let's examine the temperature distribution without the lower and upper disks, leaving only a central disk as shown in the Tank 3 configuration in Figure 7. At the bottom of the tank, where the HTF enters, four smaller vortices appear. According to the results, good mixing occurs in the lower part of the central disk compared to the upper part. This is because the warm flow of water collides with the central disk, and the resulting vortices enhances mixing. However, in the upper part of the disk, as in the previous cases, the warmer fluid is distributed along the wall, and mixing in the central part is not as effective. Calculations were carried out up to 240 s, and the results presented in Figure 6 correspond to this time.

To evaluate the evolution of the temperature distribution, Figure 7 presents the time-dependent temperature contours for the specified configurations. The previous analysis of the effect of disk arrangement on mixing efficiency is confirmed by the results presented in Figures 8-10. For instance, Figure 8 illustrates how the fluid flow evolves over time, showing that the temperature along the wall is higher compared to other areas. The formation of primary and secondary vortices is also clearly observed in this figure. Figures 8 and 9 indicate that when the lower disk is positioned close to the inlet, the maximum temperature is concentrated along the wall. This configuration is not ideal for achieving uniform mixing throughout the entire volume of the tank. In contrast, Figure 10 demonstrates that the HTF jet from the inlet collides with the central disk, leading to the formation of primary and secondary vortices that enhance mixing. Visual analysis suggests that Tank 3 is more suitable for efficient mixing. However, to draw definitive conclusions, it is necessary to perform a detailed CFD analysis. Therefore, the three configurations are further evaluated using performance indicators (13)-(23).

Figures 8-10 presents the results of calculations for the three tank configurations based on the capacity ratio parameter, calculated using Equations (13)-(15). This parameter indicates the effectiveness of each tank configuration in retaining heat within the specified temperature range of 20 °C to 50 °C. According to the results, Tank 3 achieves the highest capacity ratio
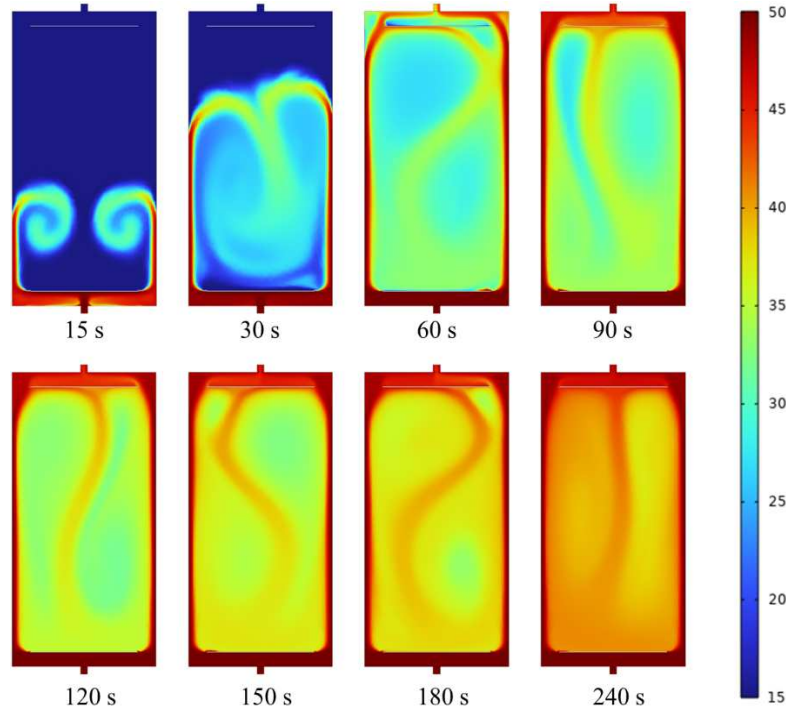
Figure 8: Temperature distribution over time: Tank 1

(σ) at 90.12%, followed by Tank 1 with 87.14%, and Tank 2 with 84.14%. As mentioned previously, when discussing Equations (16)-(18), exergy serves as an indicator of the quality of the stored thermal energy in the tank. For this parameter, Tank 3 exhibits superior performance at 81.67%, followed by Tank 1 at 76.50%, and Tank 2 at 71.50%.

The tail factor, as defined by Equation (20), serves as an indicator for assessing the quality of heat retention by the tank during long-term storage after charging. The cut-off temperature, according to Equation (19), assists in halting the charging and discharging processes promptly to prevent superheating or subcooling. However, these equations focus solely on the outlet temperature and do not account for the thermophysical properties of the fluid, tank geometry, or operating conditions. Since our analysis is centered on the quality of heat storage within the tank, the results of these calculations are not presented.

The Richardson number defined by Equation (23) characterizes the balance between buoyancy and inertial effects in a flow. A higher Richardson number indicates a greater influence of buoyancy on the flow. This analysis aids in understanding how the temperature distribution in the tank evolves and how various parameters impact heat transfer efficiency. In simpler terms, a lower Richardson number signifies better mixing. Additionally, the Richardson number should change smoothly over time without abrupt variations. Figure 12 shows the time distribution of the Richardson number for the three tank configurations. The initial values of the Richardson number ((Ri)) for all three cases are approximately 2. A sharp decrease in (Ri) is observed during the first 50 seconds, indicating intense mixing and a rapid decrease in the temperature difference between T_{top} and T_{bottom} within the tank.

After the initial sharp decrease, (Ri) declines more gradually. The different curves exhibit
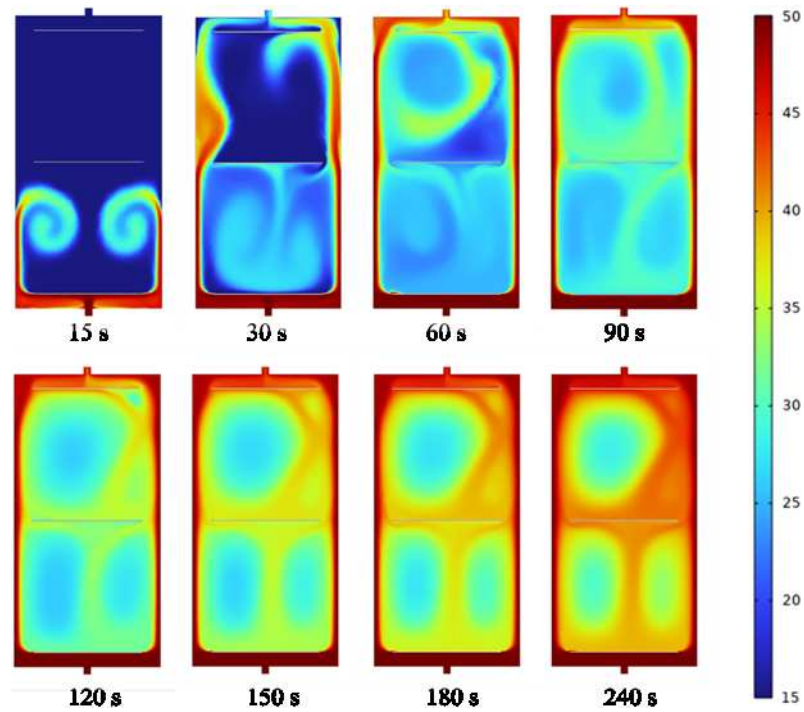
Figure 9: Temperature distribution over time: Tank 2
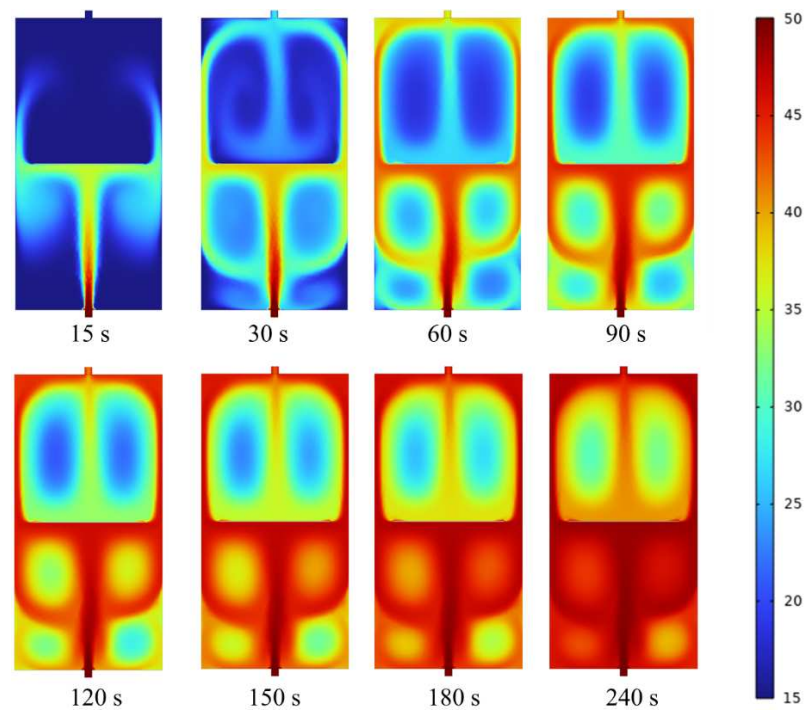
Figure 10: Temperature distribution over time: Tank 3
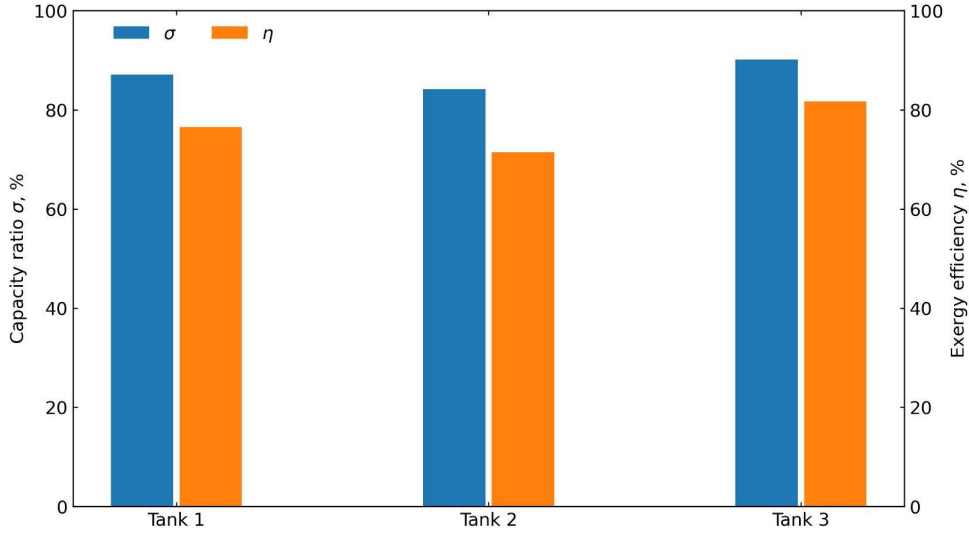
Figure 11: Comparison of capacity ratios and exergy efficiencies for the tanks.

similar trends with some variations:(Ri) for Tank 1 decreases more rapidly and stabilizes at a lower level, where as (Ri) for Tank 3 maintains a comparatively higher value with a smoother change. A smooth change in the Richardson number indicates that stratification is being disrupted and mixing is improving. Among the three tanks, Tank 3 demonstrates the best mixing results. The curves show a gradual decrease and tend to stabilize around values of 0.2-0.4. This indicates a reduction in temperature difference and the establishment of a more uniform temperature distribution along the height of the tank. For Tank 1 and Tank 2, the use of disks causes asymmetrical vortex flows near the inlet and outlet openings. This affects the oscillatory nature of the Richardson number changes for these cases, as shown in Figure 12. These oscillations indicate uneven mixing in these tanks. Thus, the Richardson number analysis also confirms that Tank 3 is the most suitable option for achieving uniform temperature distribution in the tank.

The following are the results for the charging efficiency of the thermal accumulator according to Equation (21). The discharge efficiency, calculated using Equation (22), shows a similar trend. According to the calculation results, the maximum charging efficiency is achieved by Tank 3 with a value of 67.51%, followed by Tank 2 with 64.84% and Tank 1 with 52.1%. An important factor in these indicators is that the coolant outlet temperature is always considered. Essentially, charging efficiency is influenced by the water's inlet and outlet temperatures. For comparison, when calculating the capacity ratio using Equations (13)-(15), the outlet temperature T_{out} is not taken into account, as if a tank with a plug is considered. In practice, when charging the tank, the HTF's inlet and outlet are organized. If the capacity ratio reflects the more theoretical capabilities of the tank, then the charging efficiency is a practical indicator of performance. For example, in the case of Tank 3, 67.51% of the incoming heat can be effectively stored in the tank. According to the charging and discharging efficiency parameters, Tank 3 also demonstrates better results compared to the other two configurations.
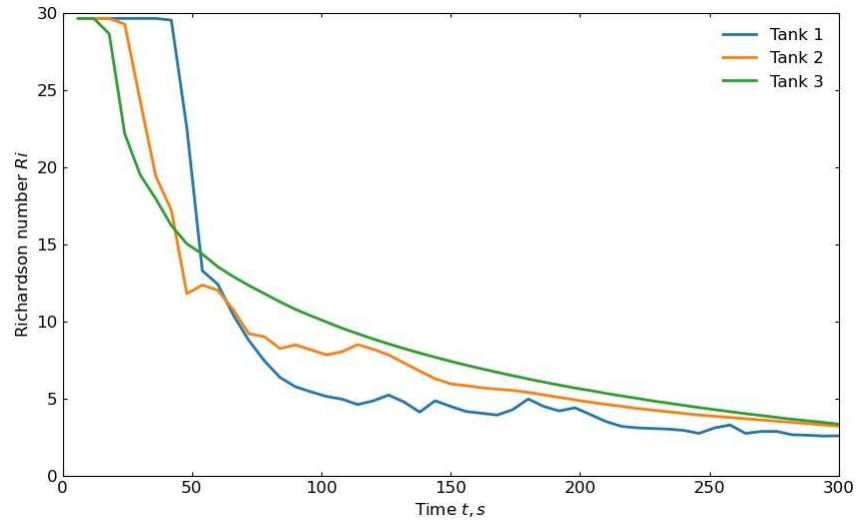
Figure 12: Time evolution of the Richardson number for the tanks.

6 Conclusions

A two-dimensional mathematical model with appropriate initial and boundary conditions for a tank containing internal disk-shaped obstacles has been developed. The calculation algorithm utilizes the built-in solvers of the licensed COMSOL Multiphysics 5.6 software. The COMSOL model demonstrates a maximum difference of 2.2% from experimental results and an even smaller difference compared to ANSYS Fluent. These findings indicate that the COMSOL algorithm accurately captures the charging and discharging processes of a sensible heat storage tank with internal obstacles.

Using the validated calculation algorithm, numerical studies were conducted to analyze the temperature distribution and performance indicators for three different tank configurations. In this analysis, Tank 3 consistently outperformed Tanks 1 and 2 across several performance indicators. It demonstrated superior mixing efficiency, as indicated by smoother changes in the Richardson number and a more uniform temperature distribution. Tank 3 also achieved the highest capacity ratio (90.12%) and exergy efficiency (81.67%), reflecting its effectiveness in heat retention and quality of stored thermal energy. Additionally, Tank 3 showed the highest charging efficiency at 67.51%, indicating its ability to store incoming heat more effectively. These results confirm that Tank 3 is the most efficient configuration for thermal energy storage and uniform temperature distribution.

7 Acknowledgments

8 Funding

Nomenclature

$\dot{m}$	Mass flow rate, kg/s;
C_p	Heat capacity, J/kg°C;
T	Temperature, °C;
T^*	Dimensionless temperature;
u, v	Velocity components, m/s;
k	Thermal conductivity, W/mK;
E	Energy, J;
F	Gravity, N;
P	Pressure, Pa;
H	Enthalpy, J;
t	Time, s;
g	Gravity, m/s^2;
β	Coefficient of thermal expansion;
ρ	Density, kg/m^3;
μ	Dynamic viscosity, kg/ms;
τ	Tail factor;
Ri	Richardson number;
D	Diameter of tank, m;
d	Diameter of metal disc, m;
b	Diameter of inlet/outlet orifices, m;
H	Height of tank, m;
h	Height of the metal disc, m;
V	Volume, m^3;
error	Relative error;

Subscripts

f	Heat transfer fluid;
y	Vertical direction;
h	Hot water;
c	Cold water;
ini	Initial value;
in	Inlet quantity;
out	Outlet quantity;
top	Top layer;
bottom	Bottom layer;

exp   Experimental value;
num   Numerical value;

Abbreviations

TES   Thermal Energy Storage;
HTF   Heat Transfer Fluid;
CFD   Computational Fluid Dynamics;
H&M   Heat and Mass Transfer;
FDM   Finite Difference Method;
FEM   Finite Element Method;
FVM   Finite Volume Method;

References

[1] Chandra Y.P., Matuska T. Stratification analysis of domestic hot water storage tanks: A comprehensive review. //Energy and Buildings – 2019.– vol.187, pp. 110-131.

[2] Fertahi S.E.-D., Jamil A., Benbassou A. Review on Solar Thermal Stratified Storage Tanks (STSST): Insight on stratification studies and efficiency indicators //Energy and Buildings – 2018.– vol.176, pp. 126-145.

[3] Langerova E., Matuska T. One-dimensional modelling of sensible heat storage tanks with immersed helical coil heat exchangers: A critical review. //Journal of Energy Storage – 2023.– vol. 72, part C, no. 108507.

[4] Chekifi T., Boukraa M. CFD applications for sensible heat storage: A comprehensive review of numerical studies. //Journal of Energy Storage – 2023.– vol. 68, no. 107893.

[5] Al-abidi A.A., Bin S. Mat, Sopian K., Sulaiman M.Y., Mohammad Th.A.CFD applications for latent heat thermal energy storage: a review. //Renewable and Sustainable Energy Reviews– 2023.– vol. 20, pp. 353-363.

[6] Rendall J., Abu-Heiba A., Gluesenkamp K., Nawaz K., Worek W., Elatar A. Nondimensional convection numbers modeling thermally stratified storage tanks: Richardson's number and hot-water tanks. //Renewable and Sustainable Energy Reviews– 2021.– vol. 150, no. 111471.

[7] Bouhal T., Fertahi S., Agrouaz Y., El Rhafiki T., Kousksou T., Jamil A. Numerical modeling and optimization of thermal stratification in solar hot water storage tanks for domestic applications: CFD study. //Solar Energy– 2017.– vol. 157, pp. 441-455.

[8] Fertahi S.E., Bouhal T., Kousksou T., Jamil A., Benbassou A. Experimental study and CFD thermal assessment of horizontal hot water storage tank integrating Evacuated Tube Collectors with heat pipes. //Solar Energy– 2018.– vol. 170, pp. 234-251.

[9] Lou W., Xie B., Aubril J., Fan Y., Luo L., Arriva A. Optimized flow distributor for stabilized thermal stratification in a single-medium thermocline storage tank: A numerical and experimental study. //Energy – 2023.– vol. 263, part A, no. 125709.

[10] Shafieian A., Bahrami H.R., Roostaee A., Feyzi S.S. Effects of different inlet configurations on the performance of solar storage tanks: A three-dimensional unsteady CFD simulation. //Case Studies in Thermal Engineering – 2023.– vol. 45, no. 103019.

[11] Kong L., Yuan W., Zhu N. CFD Simulations of Thermal Stratification Heat Storage Water Tank with an Inside Cylinder with Openings. //Procedia Engineering – 2023.– vol. 146, pp. 394-399.

[12] Kumar K., Singh S. Investigating thermal stratification in a vertical hot water storage tank under multiple transient operations.//Energy Reports– 2021.– vol. 7, pp. 7186-7199.

[13] Li C., He W., Bai Y., Wang J. A semi-analytic method for buoyancy-induced thermal stratification in hot water tanks during standby periods. //Applied Thermal Engineering – 2024.– vol. 249, no. 123440.

[14] COMSOL Multiphysics version 5.6.

[15] Lou W., Fan Y., Luo L. Single-tank thermal energy storage systems for concentrated solar power: Flow distribution optimization for thermocline evolution management. //Energy Storage– 2020.– vol. 32, no. 101749.

[16] Li G. Sensible heat thermal storage energy and exergy performance evaluations. //Renewable and Sustainable Energy Reviews– 2016.– vol. 53, pp. 897-923.

[17] Shah L.J., Furbo S. Entrance effects in solar storage tanks.//Solar Energy– 2003.– vol. 75, pp. 337-348.

[18] Bai Y., Wang Z., Fan J., Yang M., Li X., Chen L., Yuan G., Yang J. Numerical and experimental study of an underground water pit for seasonal heat storage. //Renewable Energy – 2020.– vol. 150, pp. 487-508.

[19] El-Amin M.F., Al-Ghamdi A. Experiments and numerical simulation for a thermal vertical jet into a rectangular water tank. //Results in Physics – 2018.– vol. 10, pp. 680-692.

[20] Modi A., Pĕrez-Segarra C.D. Thermocline thermal storage systems for concentrated solar power plants: One dimensional numerical model and comparative analysis. //Solar Energy – 2014. – vol. 100, pp. 84-93.

[21] Fasquelle T., Falcoz Q., Neveu P., Hoffmann J.-F. A temperature threshold evaluation for thermocline energy storage in concentrated solar power plants.//Applied Energy – 2018. – vol. 212, pp. 1153-1164.

[22] Zachar A., Farkas I., Szlivka F. Numerical analyses of the impact of plates for thermal stratification inside a storage tank with upper and lower inlet flows. //Solar Energy – 2003. – vol. 74, pp. 287-302.

Information about authors:

Alina Abdidin – a 2nd-year master's student of the dual-degree program between Al-Farabi Kazakh National University (Kazakhstan) and the University of Lorraine (France) in the specialty "7M05405 - Mechanics and Energy". Recipient of the one-year Eiffel scholarship from the Ministry of Europe and Foreign Affairs of the French Republic (Almaty, Nancy, Kazakhstan, France, alina.abdidin1@etu.univ-lorraine.fr; alinaab808@gmail.com);

Aiym Kereikulova – a 2nd-year master's student of the dual-degree program between Al-Farabi Kazakh National University (Kazakhstan) and the University of Lorraine (France) in the specialty "7M05405 - Mechanics and Energy". Recipient of the one-year Abai-Verne scholarship under the joint program of the Ministry of Science and Higher Education of the Republic of Kazakhstan and the Ministry of Europe and Foreign Affairs of the French Republic (Almaty, Nancy, Kazakhstan, France, aiym.kereikulova9@etu.univ-lorraine.fr; aiymkereikulova56@gmail.com);

Amankeldy Toleukhanov – PhD, Associate Professor of the Department of Mechanical Engineering at Satbayev University (Almaty, Kazakhstan, aman.toleukhanov@gmail.com);

Olivier Botella – PhD, Associate Professor at the University of Lorraine, France. Researcher at the "Heat Management"Lab of the Energy, Theoretical and Applied Mechanics Research Center (LEMTA), University of Lorraine, France. Coordinator of the dual-degree program (from the French side) between Al-Farabi Kazakh National University and the University of Lorraine in the specialty "7M05405 - Mechanics and Energy"(Nancy, France, olivier.botella@univ-lorraine.fr);

Abdelhamid Kheiri – PhD, Associate Professor at the University of Lorraine, France. Researcher at the "Heat Management"Lab of the Energy, Theoretical and Applied Mechanics Research Center (LEMTA), University of Lorraine, France (Nancy, France, abdelhamid.kheiri@univ-lorraine.fr);

Yerzhan Belyayev (corresponding author) –PhD, Associate Professor, Acting Professor of the Department of Mechanics at Al-Farabi Kazakh National University. Coordinator of the dual-degree program (from the Kazakh side) between Al-Farabi Kazakh National University and the University of Lorraine in the specialty "7M05405 - Mechanics and Energy"(Almaty, Kazakhstan, yerzhan.belyaev@kaznu.edu.kz; yerzhan.belyayev@gmail.com).

Авторлар туралы мәлімет:

Абдидин Алина Нұрлыбекқызы – әл-Фараби атындағы Қазақ ұлттық университеті (Қазақстан) мен Лотарингия университеті (Франция) арасындағы қос дипломды бағдарламаның, "7М05405 - Механика және энергетика"мамандығы бойынша 2-курс магистранты. Францияның, Еуропа және Сыртқы істер министрлігі тарапынан берілетін Эйфель (Eiffel) бір жылдық стипендиясының иегері (Алматы қаласы, Нанси қаласы, Қазақстан, Франция, alina.abdidin1@etu.univ-lorraine.fr; alinaab808@gmail.com);

Керейқұлова Айым Есенқұлқызы – әл-Фараби атындағы Қазақ ұлттық университеті (Қазақстан) мен Лотарингия университеті (Франция) арасындағы қос дипломды бағдарламаның, "7М05405 - Механика және энергетика"мамандығы бойынша 2-курс магистранты. Қазақстан Республикасы Ғылым және Жоғары білім министрлігі мен Францияның Еуропа және Сыртқы істер министрлігінің бірлескен Абай-Верн бағдарламасы аясындағы бір жылдық стипендиясының иегері (Алматы қаласы, Нанси қаласы, Қазақстан, Франция, aiym.kereikulova9@etu.univ-lorraine.fr; aiymkereikulova56@gmail.com);

Төлеуханов Аманкелді Әлешұлы - PhD, Қ.И. Сәтбаев атындағы Қазақ ұлттық техникалық зерттеу университетінің Инженерлік механика кафедрасының қауымдастырылған профессоры (Алматы қаласы, Қазақстан, aman.toleukhanov@gmail.com).;

Оливье Ботелла - PhD, Лотарингия университетінің қауымдастырылған профессоры. Лотарингия университеті жанындағы "Жылу менеджменті"зертханасының LEMTA атты энергетика, теориялық және қолданбалы механика зерттеу орталығының ғылыми қызметкері. әл-Фараби атындағы Қазақ ұлттық университеті мен Лотарингия университеті арасындағы "7М05405 - Механика және энергетика"мамандығы бойынша қос дипломды бағдарламаның Француз тарапынан координаторы (Нанси қаласы, Франция, olivier.botella@univ-lorraine.fr);

Абдельхамид Хеири - PhD, Лотарингия университетінің қауымдастырылған профессоры. Лотарингия университеті жанындағы "Жылу менеджменті"зертханасының LEMTA атты энергетика, теориялық және қолданбалы механика зерттеу орталығының ғылыми қызметкері. (Нанси қаласы, Франция, abdelhamid.kheiri@univ-lorraine.fr);

Беляев Ержан Келесұлы (корреспондент автор) - PhD, қауымдастырылған профессор, әл-Фараби атындағы Қазақ ұлттық университетінің Механика кафедрасының профессор міндетін атқарушы. әл-Фараби атындағы Қазақ ұлттық университеті мен Лотарингия университеті арасындағы "7М05405 - Механика және энергетика"мамандығы бойынша қос дипломды бағдарламаның Қазақ тарапынан координаторы (Алматы қаласы, Қазақстан, yerzhan.belyaev@kaznu.edu.kz; yerzhan.belyayev@gmail.com).